INDONESIAN JOURNAL ON GEOSCIENCE
Geological Agency
Ministry of Energy and Mineral Resources

Journal homepage: http://ijog.geologi.esdm.go.id
ISSN 2355-9314, e-ISSN 2355-9306

Petrography and Mineral Chemistry of Magmatic and Hydrothermal Biotite in Porphyry Copper-Gold Deposits: *A Tool for Understanding Mineralizing Fluid Compositional Changes During Alteration Processes*

Arifudin Idrus

Department of Geological Engineering, Universitas Gadjah Mada
Jln. Grafika No. 2 Bulaksumur, Yogyakarta 55281, Indonesia

Corresponding author: arifidrus@ugm.ac.id
Manuscript received: May 29, 2017; revised: August 12, 2017;
approved: January 23, 2018; available online: February 15, 2018

Abstract - This study aims to understand the petrography and chemistry of both magmatic and hydrothermal biotites in porphyry copper-gold deposits, and to evaluate the fluid compositional changes during alteration processes. A total of 206 biotite grains from selected rock samples taken from the Batu Hijau porphyry Cu-Au deposit was analyzed. Detailed petrography and biotite chemistry analysis were performed on thin sections and polished thin sections, respectively, representing various rocks and alteration types. A JEOL JXA-8900R electron microprobe analyzer (EMPA) was used for the chemistry analysis. The biotite is texturally divided into magmatic and hydrothermal types. Ti, Fe, and F contents can be used to distinguish the two biotite types chemically. Some oxide and halogen contents of biotite from various rocks and alteration types demonstrate a systematic variation in chemical composition. Biotite halogen chemistry shows a systematic increase in log (X_{Cl}/X_{OH}) and decrease in log (X_F/X_{OH}) values from biotite (potassic) through chlorite-sericite (intermediate argillic) to actinolite (inner propylitic) zones. The *y*-intercepts on the log (X_{Cl}/X_{OH}) *vs*. X_{Mg} and log (X_F/X_{OH}) *vs*. X_{Fe} plotted for biotite from potassic and intermediate argillic zones are similar or slightly different. In contrast, the *y*-intercepts on the log (X_{Cl}/X_{OH}) *vs*. X_{Mg} and log (X_F/X_{OH}) *vs*. X_{Fe} plotted for biotite from inner propylitic zone display different values in comparison to the two alteration zones. Halogen (F,Cl) fugacity ratios in biotite show a similar pattern: in the potassic and intermediate argillic zones they show little variation, whereas in the inner propylitic zone they are distinctly different. These features suggest the hydrothermal fluid composition remained fairly constant in the inner part of the deposit during the potassic and intermediate argillic alteration events, but changed significantly towards the outer part affected by inner propylitic alteration. High halogen content, particularly Cl, in hydrothermal biotite may portray that copper and gold were transported in mineralizing fluids in the form of chloride complexes $CuCl_2^-$ and $AuCl_2^-$, respectively.

Keywords: biotite, fluid composition change, halogen F and Cl, mineral chemistry, petrography, porphyry Cu-Au deposits

How to cite this article:
Idrus, A., 2018. Petrography and Mineral Chemistry of Magmatic and Hydrothermal Biotite in Porphyry Copper-Gold Deposits: A Tool for Understanding Mineralizing Fluid Compositional Changes During Alteration Processes. *Indonesian Journal on Geoscience*, 5 (1), p.47-64. DOI: 10.17014/ijog.5.1.47-64

Introduction

Biotite, a trioctahedral mica with the generalized formula (K, Na, Ca, Ba) (Fe^{+2}, Fe^{+3}, Mg, Ti^{+4}, Mn, Al)$_3$ (Al, Si)$_4O_{10}$(OH, F, Cl)$_2$ is a common constituent in many porphyry copper deposits. In such environment, most biotite has formed during igneous crystallization of the host intrusive

or during hydrothermal alteration of the plutonic host. Since many thermodynamic variables can control the complex chemistry of biotite, its composition is potentially useful in understanding some of the physical and chemical conditions associated with igneous and hydrothermal events leading to the formation of the porphyry copper deposits.

The majority of previous studies of biotite chemical composition in porphyry Cu deposits have concentrated on the F and Cl mineral contents, with the objective of distinguishing between mineralized and barren plutons. Few studies of porphyry Cu deposits have reported full elemental chemistry of biotite. A notable exception is the study by Parry and Jacobs (1975) who reported variations in biotite chemistry from potassic, phyllic, propylitic, and argillic alteration zones in Santa Rita deposit, and estimated the HF, HCl, and H_2O fugacity of hydrothermal fluids. Selby and Nesbitt (2000) published the chemical composition of biotite from Casino porphyry Cu-Au-Mo mineralization and an evaluation of magmatic and hydrothermal fluid chemistry. Our knowledge of the HF, HCl, and H_2O fugacity of hydrothermal fluids associated with porphyry Cu mineralization and hydrothermal alteration is based on limited published thermodynamic data (Parry and Jacobs, 1975; Parry *et al*., 1978; Munoz and Swenson, 1981; Munoz, 1984; Loferski and Ayuso, 1995). Presently, there are several studies dealing with mineral chemistry of hydrothermal biotite from numerous porphyry copper deposits worldwide, such as Kahang deposit, Iran (Afshooni *et al*., 2013), Lar deposit, Iran (Moradi *et al*., 2016), Dexing deposit, China (Bao *et al*., 2016), and Sisson Brook deposit, New Brunswick, Canada (Zhang *et al*., 2016). Halogen chemistry of magmatic biotite within the mineralization-bearing tonalite porphyry in Batu Hijau deposit, Indonesia, was described by Idrus *et al*. (2007).

This study comprises detailed petrographic examination and microprobe analysis of the major and minor element chemistry of various biotite types, particularly hydrothermal biotite, together with evaluation of hydrothermal fluid changes during alteration processes of the porphyry copper-gold deposits based on a case study of the Batu Hijau deposit.

The Batu Hijau porphyry Cu-Au deposit is located in the southern part of Sumbawa Island, Indonesia (Figure 1). It contains 914 million metric tonnes of ore at an average grade of 0.53% Cu and 0.40 g/t Au (Clode *et al*., 1999). The wall rock units of the deposit consist of interbedded andesitic lithic breccia and fine-grained volcaniclastic rocks as well as intrusions of porphyry andesite and quartz diorite bodies. These units are intruded by multiple phases of tonalite porphyry stocks. Copper and gold mineralization is directly related to the emplacement of the tonalite porphyries. Hydrothermal alteration and mineralization developed in four temporally and spatially overlapping stages include (1) early alteration stage divided into biotite (potassic), actinolite (inner propylitic), and chlorite-epidote (outer propylitic) zones, (2) transitional alteration stage typified by a chlorite-sericite (intermediate argillic) zone, (3) late alteration stage characterized by the destruction of feldspar and the formation of pyrophyllite-andalusite (advanced argillic) and sericite-paragonite (argillic) zones, and (4) very late alteration stage consisting of illite-sericite replacement of feldspar (Idrus, 2005).

Research Methods

A suite of representative thin section and polished thin section samples from the Batu Hijau porphyry copper-gold deposit was petrographically observed. A total of 206 biotite grains from selected rock samples was analyzed chemically. All elemental analysis of biotites was obtained from polished thin section using a JEOL JXA-8900R electron microprobe at Institute of Mineralogy and Economic Geology, RWTH Aachen University, Germany. Each analysis was classified according to the textural type of the biotite and to the kind of rock and the type of alteration of which the biotite is associated.

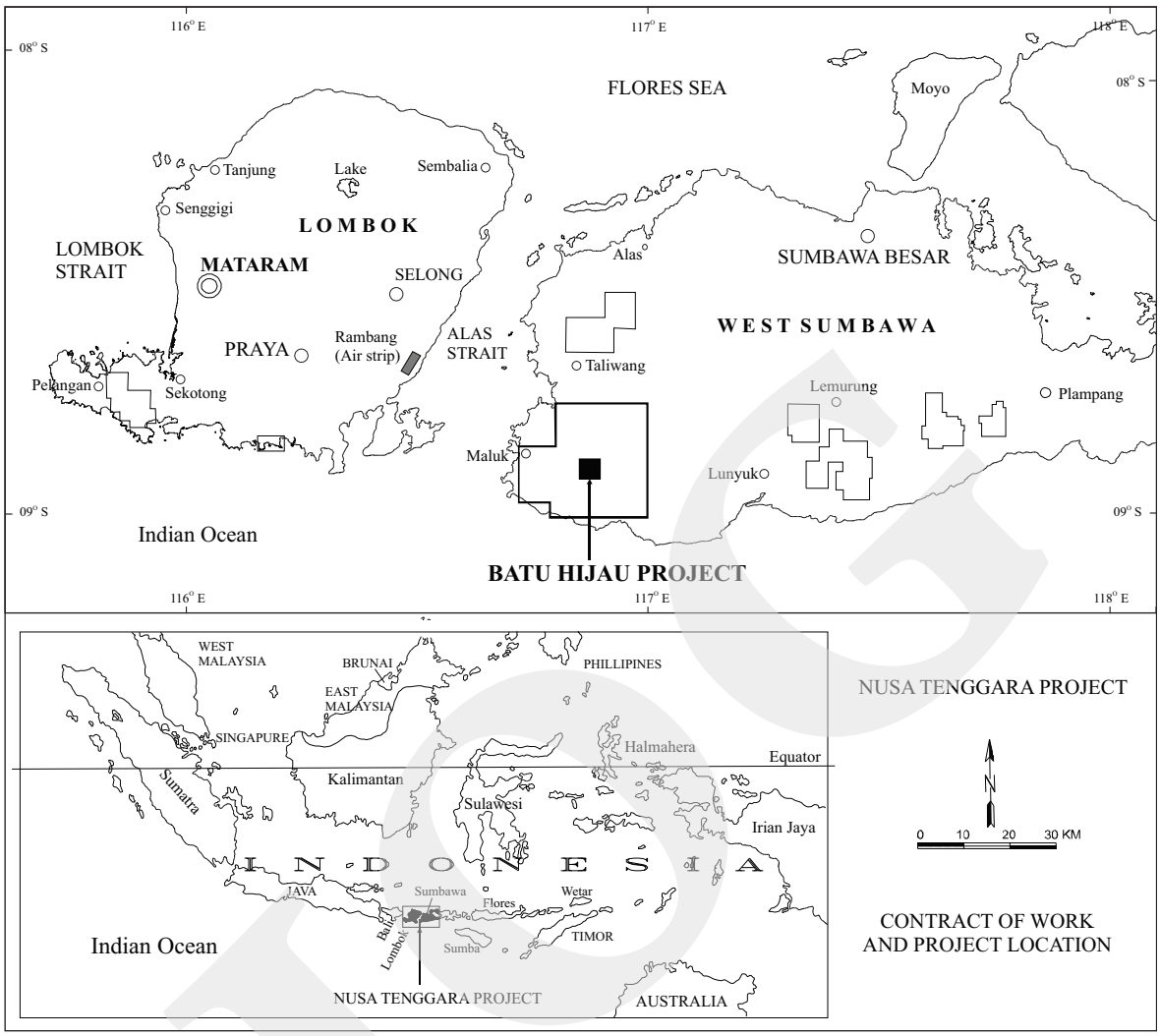

Figure 1. Location of the Batu Hijau porphyry copper-gold deposit in Sumbawa Island, Indonesia.

Element determinations (Si, Ti, Al, Fe_{Total}, Mn, Mg, Ca, Na, K, F, and Cl) were carried out using a beam size of 1.6 μm, an accelerating potential voltage of 15 kV, a probe current of 23.5 nA, and a counting time of 10 s for each element analyzed. Ba was not analyzed due to very low concentration of the element. The analytical procedure for Si, Ti, Al, Fe, Mn, Mg, Ca, Na, K, F, and Cl used synthetic standards of plagioclase (Pl_{64}), rutile ($Ru_{83}Ti_3P$), spinel ($Sp_{761}T$), fayalite ($Fa_{66}Mn$), jadeite (J_{107}), orthoclase (Or_{79}), fluorite ($F_{180}TAP$), and tugtupite (Tug_{34}). Matrix effects were corrected using the ZAF software provided by JEOL. The accuracy of the reported values for the analysis is 0.2%-15% (1σ) depending on the abundance of the element. A microprobe analysis was defined as the value of one spot analysis of biotite grain. The OH values were calculated on the basis of eleven oxygen formula units. The X_{phl} (mole fraction phlogopite), $X_{Mg,}$ and X_{Fe} values were determined from cation fractions and defined as Mg/(sum of octahedral cations), Mg/(Fe+Mg), and $(Fe/Al^{IV})/(Mg+Fe+Al^{VI})$, respectively (Zhu and Sverjensky, 1992; Loverski and Ayuso, 1995). The X_F, X_{Cl}, and X_{OH} are the mole fractions of F, Cl, and OH in the hydroxyl site. The halogen fugacity ratios consisting of log $(fH_2O)/(fHF)$, log $(fH_2O)/(fHCl)$, and log $(fHF)/(fHCl)$ were computed using the equations of Munoz (1992), which were based on the revised coefficients for the halogen-hydroxyl exchange (Zhu and Sverjensky, 1991, 1992).

Results and Discussion

Biotite Petrography

At the Batu Hijau deposit, biotite grains occur in the central biotite (potassic), transitional chlorite-sericite (intermediate argillic), and proximal actinolite (inner propylitic) alteration zones. The biotites are petrographically classified as magmatic and hydrothermal types. The term "magmatic" denotes biotite grains inferred to have crystallized directly from silicate melt. In the case of the Batu Hijau deposit, the magmatic biotites are observed in both least-altered and potassic-altered tonalite samples. The magmatic biotites are texturally euhedral to subhedral, with the length ranging from 1 to 4 mm (Figure 2). Some magmatic biotites are slightly ragged, splintery, or frayed.

The term "hydrothermal" describes biotites inferred to have precipitated from the hydrothermal fluids and biotites that have partially completely replaced magmatic biotite and hornblende. The hydrothermal biotites are petrographically distinct from magmatic biotites, commonly occurring as aggregates of fine-grained flakes (typically 10-100 µm) with a crude orientation (Figure 2). Biotite grains that occur in the early veinlets/stringers are also termed "hydrothermal". This biotite type is identified in all altered rock types, including tonalite porphyries, equigranular quartz diorite, and andesitic volcaniclastic rocks.

Biotite Chemistry

A total of 172 electron microprobe analyses of 860 spot analyses of magmatic and hydrothermal biotite grains from the central biotite (potassic), transitional chlorite-sericite (intermediate argillic), and proximal actinolite (inner propylitic) alteration zones were made. In the context used here, a microprobe analysis was defined as the arithmetic mean of 5 - 10 spot analyses of a biotite grain or an aggregate of fine-grained biotites,

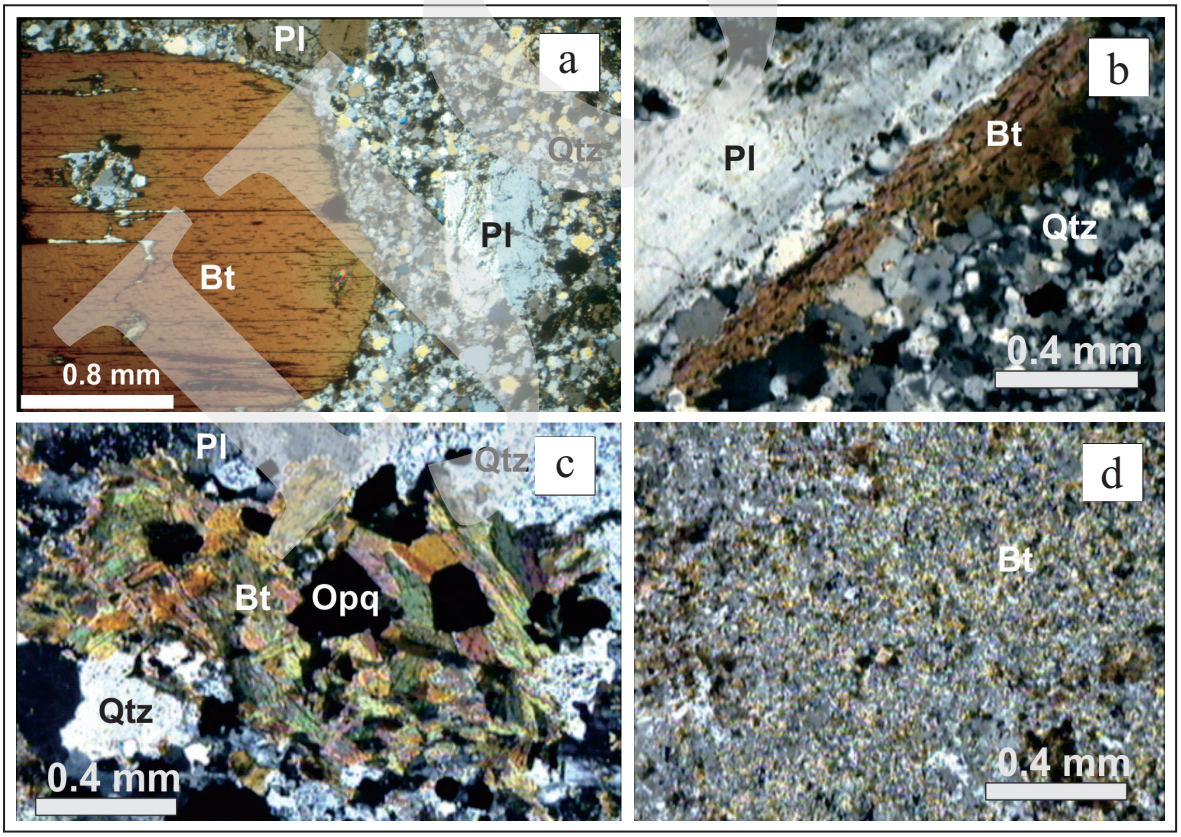

Figure 2. Biotite types: (a, b) Subhedral magmatic biotite phenocryst in young tonalite, (c) an aggregate of fine-grained flakes of hydrothermal biotite in equigranular quartz diorite, replacing the early hornblende, and (d) scattered fine-grained biotite in andesitic volcaniclastics. Mineral abbreviation: Bt = biotite, Pl = plagioclase, Qtz = quartz, and Opq = opaque mineral.

depending on the size and/or the number of grains analyzed. Representative microprobe data of biotites from different rock types and alteration zones in the Batu Hijau deposit are presented in Tables 1 and 2.

The representative electron microprobe data indicate that the magmatic and hydrothermal biotites are virtually identical and plotted in the field of phlogopite (cf. Rieder *et al.*, 1998; Figure 3). However, there are some variations in elemental

Table 1. Representative Microprobe Data of Magmatic and Hydrothermal Biotites in Least-Altered and Altered Tonalite Porphyries in The Batu Hijau Deposit

Sample	**25342-05**	**25336-07**	**25342-02**	**25338-08**	**25303-06**	**25303-07**	**25337-23**	**25337-01**	**25337-13**	**25337-02**	**25337-17**	**25337-03**
Rock Type	**Intermediate tonalite**			**Intermediate tonalite**			**Young tonalite**			**Young tonalite**		
Alteration	**-**			**Biotite (potassic)**			**-**			**Chlorite-Sericite (interm. Agrilic)**		
Origin	**Magmatic**			**Hydrothermal**			**Magmatic**			**Hydrothermal**		
SiO_2	39.597	38.732	40.018	41.084	40.749	39.497	38.542	38.966	39.987	39.388	39.848	38.359
TiO_2	3.407	3.219	3.316	2.378	2.522	2.66	3.818	3.698	3.392	2.117	1.694	2.233
Al_2O_3	14.04	13.745	13.734	13.121	13.392	13.294	13.507	13.036	13.669	12.987	14.183	13.92
FeO	12.448	13.202	10.737	10.489	10.811	11.069	12.308	11.739	12.715	10.967	10.659	11.955
MnO	0.142	0.122	0.12	0.054	0.036	0.05	0.066	0.125	0.059	0.135	0.105	0.112
MgO	17.058	16.978	17.293	19.922	19.76	18.956	17.18	17.722	16.829	20.008	19.592	19.127
CaO	Bd	Bd	0.011	Bd	0.042	0.012	Bd	0.011	0.119	0.05	0.034	0.012
Na_2O	0.185	0.197	0.171	0.155	0.212	0.196	0.255	0.203	0.329	0.302	0.149	0.136
K_2O	8.857	9.297	8.84	8.741	9.081	9.327	8.425	8.381	8.017	8.616	8.915	7.687
F	0.864	0.771	0.843	0.986	1.429	1.209	0.558	0.638	0.277	0.626	1.242	0.846
Cl	0.196	0.222	0.179	0.189	0.276	0.257	0.261	0.212	0.209	0.229	0.224	0.165
H_2O (recalc.)	3.65	3.64	3.64	3.66	3.44	3.46	3.71	3.69	3.92	3.73	3.48	3.6
Total	100.444	100.125	98.902	100.779	101.75	99.987	98.63	98.421	99.522	99.155	100.125	98.152
Element	Number of cations based on 24 (O, OH, F, Cl)											
Si	5.772	5.712	5.87	5.9	5.839	5.785	5.718	5.775	5.842	5.781	5.79	5.689
Al^{IV}	2.228	2.288	2.13	2.1	2.161	2.215	2.282	2.225	2.158	2.219	2.21	2.311
Tetrahedral	8	8	8	8	8	8	8	8	8	8	8	8
Al^{IV}	0.182	0.099	0.242	0.119	0.099	0.078	0.078	0.05	0.194	0.026	0.217	0.12
Ti	0.374	0.357	0.366	0.257	0.272	0.293	0.426	0.412	0.373	0.234	0.185	0.249
Fe*	1.517	1.628	1.317	1.26	1.295	1.356	1.527	1.455	1.554	1.346	1.295	1.483
Mn	0.018	0.015	0.015	0.007	0.004	0.006	0.008	0.016	0.007	0.017	0.013	0.014
Mg	3.707	3.732	3.781	4.265	4.221	4.139	3.8	3.195	3.665	4.378	4.244	4.229
Ca			0.002	0.001	0.006	0.002		0.002	0.019	0.008	0.005	0.002
Octahedral	5.798	5.831	5.723	5.909	5.897	5.874	5.839	5.85	5.812	6.009	5.959	6.097
Na	0.052	0.056	0.049	0.043	0.059	0.056	0.073	0.058	0.093	0.086	0.042	0.039
K	1.647	1.749	1.654	1.601	1.66	1.743	1.595	1.585	1.494	1.613	1.653	1.454
Interlayer	1.699	1.805	1.703	1.644	1.719	1.799	1.668	1.643	1.587	1.699	1.695	1.493
Anios (afu)												
F	0.797	0.719	0.782	0.896	1.295	1.12	0.524	0.598	0.256	0.581	1.141	0.794
Cl	0.097	0.111	0.089	0.092	0.134	0.128	0.131	0.107	0.104	0.114	0.11	0.083
OH (recalc.)	3.553	3.585	3.564	3.506	3.285	3.376	3.673	3.648	3.82	3.365	3.374	3.562
X_{Mg}	0.71	0.7	0.74	0.77	0.77	0.75	0.71	0.73	0.7	0.76	0.77	0.74
X_{Fe}	0.314	0.316	0.292	0.244	0.248	0.257	0.297	0.278	0.323	0.239	0.263	0.275
X_{phl}	0.639	0.640	0.661	0.722	0.716	0.705	0.651	0.669	0.631	0.729	0.712	0.694

Table 2. Representative Microprobe Data of Hydrothermal Biotite in Altered Equigranular Quartz Diorite (Qde) and Andesitic Volcaniclastics (Vxl) Wall-Rocks

Sample	25288-12	25288-13	25288-14	25287-03	25287-04	25287-05	25436-23	25436-24	25436-25	25450-24	25450-25	25450-26
Rock Type	Equigranular quartz diorite (Qde)			Equigranular quartz diorite (Qde)			Andesitic volcaniclastic (Vxl)			Andesitic volcaniclastic (Vxl)		
Alteration	Biotite (potassic)			Chlorite-sericite (interm. Argillic)			Chlorite-Sericite (interm. Agrilic)			Actinolite (inner propylitic)		
Origin	Hydrothermal			Hydrothermal			Hydrothermal			Hydrothermal		
SiO_2	39.254	38.943	38.774	37.32	39.518	39.557	37.641	38.386	38.303	38.846	38.813	38.289
TiO_2	3.623	3.893	3.689	2.197	2.147	2.252	2.534	2.648	2.422	4.917	4.169	4.411
Al_2O_3	13.634	13.497	13.532	15.078	15.198	14.974	16.795	16.037	15.484	13.365	13.318	14.131
FeO	12.015	12.038	11.876	12.668	11.165	11.327	14.345	14.163	13.46	13.676	13.918	14.099
MnO	0.172	0.191	0.148	0.146	0.116	0.134	0.083	0.072	0.04	0.346	0.391	0.41
MgO	17.722	17.878	17.068	16.95	17.783	17.904	14.257	15.315	15.904	15.312	15.401	14.875
CaO	bd	0.018	bd	0.047	0.026	0.024	0.019	bd	bd	0.021	0.048	0.015
Na_2O	0.269	0.238	0.225	0.158	0.149	0.18	0.101	0.122	0.104	0.165	0.143	0.116
K_2O	9.042	9.182	8.88	8.244	9.379	8.82	8.83	9.167	8.926	9.178	8.697	8.972
F	0.356	0.394	0.374	0.663	0.641	0.609	0.438	0.385	0.439	0.377	0.635	0.319
Cl	0.237	0.23	0.227	0.26	0.254	0.247	0.224	0.334	0.327	0.305	0.318	0.316
H_2O (recalc.)	3.88	3.86	3.81	3.6	3.75	3.77	3.77	3.82	3.75	3.81	3.66	3.81
Total	100.204	100.36	98.603	97.331	100.126	99.798	99.037	100.449	99.159	100.318	99.511	99.763
Element												
Si	5.73	5.689	5.748	5.621	5.748	5.76	5.6	5.637	5.677	5.724	5.765	5.678
Al^{IV}	2.27	2.311	2.252	2.379	2.252	2.24	2.4	2.363	2.323	2.276	2.235	2.322
Tetrahedral	8	8	8	8	8	8	8	8	8	8	8	8
Al^{IV}	0.074	0.011	0.11	0.396	0.352	0.328	0.543	0.41	0.38	0.043	0.095	0.146
Ti	0.398	0.428	0.411	0.249	0.235	0.247	0.284	0.292	0.27	0.545	0.466	0.492
Fe*	1.467	1.471	1.472	1.596	1.358	1.379	1.785	1.739	1.668	1.685	1.729	1.748
Mn	0.021	0.024	0.019	0.019	0.014	0.017	0.01	0.009	0.005	0.043	0.049	0.051
Mg	3.856	3.893	3.772	3.806	3.856	3.887	3.162	3.353	3.514	3.363	3.41	3.288
Ca	0.001	0.003		0.008	0.004	0.004	0.003	0.001		0.003	0.008	0.002
Octahedral	5.817	5.83	5.784	5.974	5.819	5.862	5.787	5.804	5.837	5.682	5.757	5.727
Na	0.076	0.067	0.065	0.046	0.042	0.051	0.029	0.035	0.03	0.074	0.041	0.033
K	1.684	1.711	1.679	1.584	1.741	1.638	1.676	1.717	1.688	1.725	1.648	1.697
Interlayer	1.76	1.778	1.744	1.63	1.783	1.689	1.705	1.752	1.718	1.772	1.689	1.73
Anios (afu)												
F	0.329	0.364	0.351	0.632	0.59	0.561	0.412	0.358	0.412	0.351	0.597	0.299
Cl	0.117	0.114	0.114	0.133	0.125	0.122	0.113	0.166	0.164	0.152	0.16	0.159
OH (recalc.)	3.777	3.761	3.768	3.618	3.642	3.659	3.737	3.738	3.712	3.748	3.622	3.771
X_{Mg}	0.72	0.73	0.72	0.7	0.74	0.74	0.64	0.66	0.68	0.67	0.66	0.65
X_{Fe}	0.286	0.276	0.295	0.332	0.307	0.305	0.424	0.391	0.368	0.339	0.348	0.366
X_{phl}	0.663	0.668	0.652	0.637	0.662	0.663	0.546	0.578	0.602	0.592	0.592	0.574

concentrations. TiO_2 and FeO tend to be higher in the magmatic biotite than in the hydrothermal type from the intermediate and young tonalites. In contrast, the concentration of F tends to be higher in hydrothermal biotites than in the magmatic type. Compositional variations of the two biotite types are shown graphically in Figure 4, involving mole fraction phlogopite (X_{Phl} = Mg/(sum of octahedral cations) (Zhu and Sverjensky, 1991) and weight percent of TiO_2, FeO, and F. Separate plots (not shown here) also indicate that the magmatic biotites have relative lower SiO_2

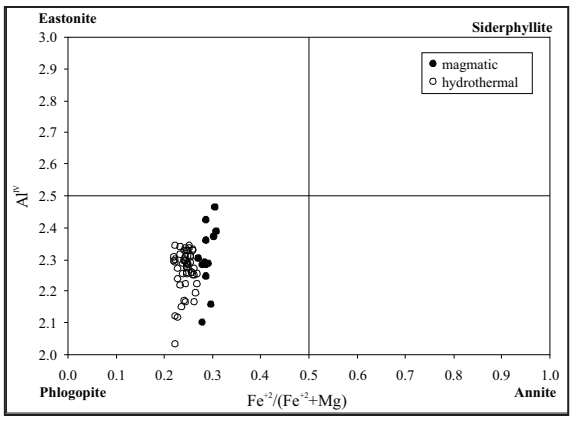

Figure 3. Magmatic and hydrothermal biotites (N = 75) in tonalite porphyries identified as phlogopite (Mg-rich biotite) (cf. classification of Rieder *et al*., 1998).

and higher Al_2O_3 values than the hydrothermal variety. However, Cl content does not appear to differ between both biotite types.

The X_{Mg} of magmatic biotite is lower than that of hydrothermal biotite. With respect to the rock types, X_{Mg} of secondary biotites in andesitic volcaniclastic rocks from various alteration zones tends to be lower ($X_{Mg} \leq 0.70$) than in intrusive rocks ($X_{Mg} > 0.70$). Secondary biotites in tonalite porphyries (intermediate and young tonalites) contain the highest X_{Mg} with an average value of 0.75, relative to those in equigranular quartz diorite (X_{Mg} = 0.73). Compositional trends between the secondary biotites in equigranular quartz diorite and andesitic volcaniclastic rocks associated with different zones of alteration are shown in a series of variation diagrams (Figure 4). Hydrothermal biotite hosted by equigranular quartz diorite shows an increase in Al_2O_3, FeO, and Cl, but a decrease in TiO_2, MnO, and F from the central biotite and transitional chlorite-sericite to proximal actinolite alteration zones. SiO_2, MnO, and F display a positive correlation with X_{Phl}, whereas the Al_2O_3, FeO, and Cl are negatively correlated with X_{Phl}.

Hydrothermal biotite in the andesitic volcaniclastic rocks shows an increase in TiO_2, Al_2O_3, FeO, MnO, and Cl, and a decrease in SiO_2 and F from the inner part (central early

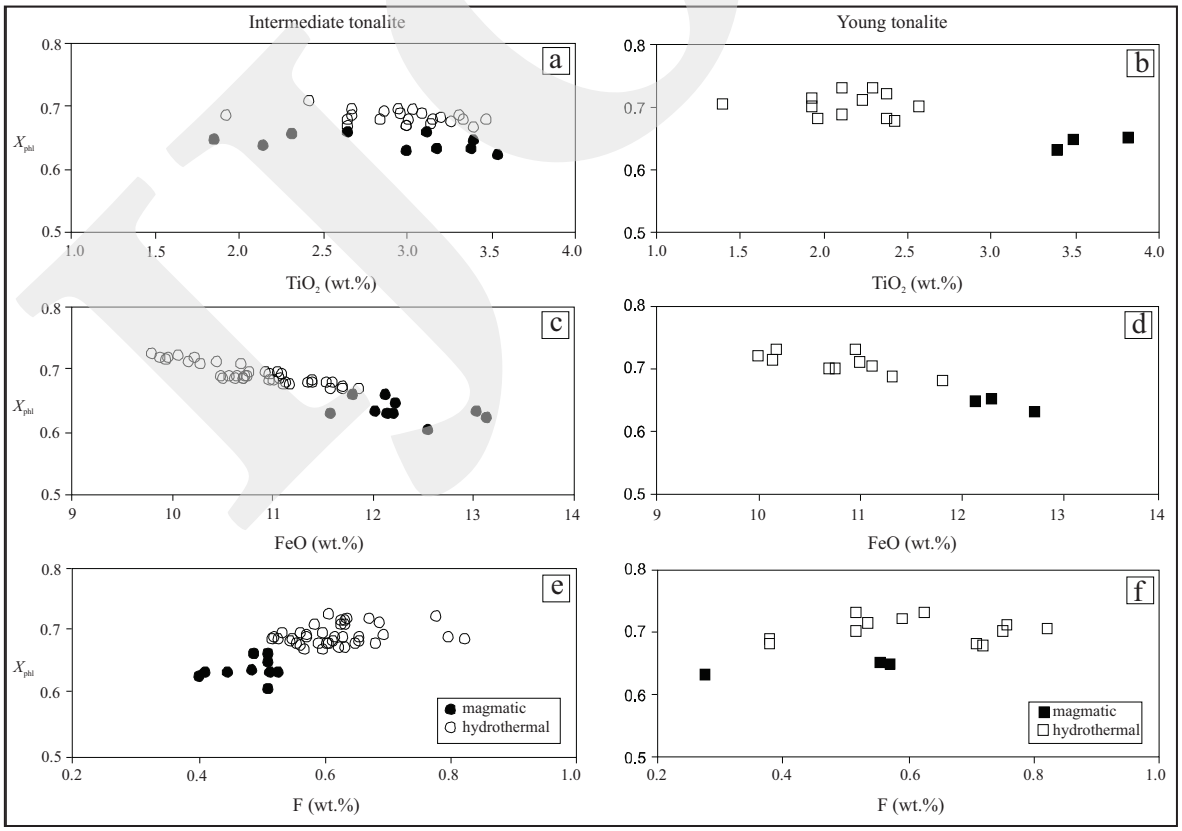

Figure 4. X_{Phl} against TiO_2, FeO, and F plots distinguishing magmatic biotite from hydrothermal biotite (N=75) in the tonalite porphyries. N = Number of biotite grains analyzed.

biotite), through the transitional chlorite-sericite (intermediate argillic) to the outer part (proximal early actinolite) zones. The TiO_2 content of biotite from the actinolitic-altered rocks is typically higher (> 3 wt.%) than in other alteration zones (< 3 wt.%), as are FeO and MnO (> 13 and 0.35 wt.%, respectively) (Figure 5). The plotting chemical data of hydrothermal biotite from actinolitic-altered andesitic volcaniclastic rocks show a different pattern compared to those of other alteration types, which may strongly be influenced by alteration intensity. Actinolitic-altered andesitic volcaniclastic rocks are relatively weak altered compared to other alteration types. Thus, some elements such as TiO_2, FeO, and MnO are preserved and remain to be high. The X_{Phl} is positively correlated with SiO_2 and F, and negatively with FeO, MnO, and Cl. Na_2O and K_2O contents show relatively similar behaviour. Some elemental concentrations in biotite in the central biotite and transitional chlorite-sericite zones are very similar, which may reflect the strong overlapping between the two alteration styles. SiO_2 and TiO_2 do not show a systematic compositional trend. However, in general, the hydrothermal biotite grains indicate a systematic compositional variation from the centre to the periphery of the deposit. The correlation between X_{Phl} and halogens (F, Cl) in all alteration zones and rock types (Figure 4a - e and Figure 5k - n) agrees well with the experimental results of Munoz (1984). It clearly demonstrates that biotites with high Mg tend to incorporate more F and less Cl in comparison to biotites with lower Mg; a crystal-chemical effect referred to as "Fe-F and Mg-Cl avoidance rules" (Munoz, 1984; Zhu and Sverjensky, 1991; Munoz, 1992). This suggests that the octahedral Mg and Fe of biotite control the halogen-hydroxyl exchange of hydrothermal fluids within the Batu Hijau deposit.

Biotite Halogen Chemistry

The halogen contents of the hydrothermal biotites are illustrated in Figure 6. The contents in different rock types are grouped according to their related alteration zones. The biotites from the central biotite, transitional chlorite-sericite, and proximal actinolite alteration zones have average log (X_{Cl}/X_{OH}) values of -1.54, -1.53, and -1.43, respectively. The log (X_F/X_{OH}) values are -0.89, -0.96, and -1.34, whereas log (X_{Cl}/X_F) values vary from 0.65, 0.58 to 0.09. The systematic variation of the logarithmic ratios reflects a systematic variation of the halogen content in biotites associated with these alteration zones.

Zhu and Sverjensky (1992) have shown that the composition of biotite formed under similar physicochemical conditions produces linear trends on log (X_F/X_{OH}) against X_{Fe} and log (X_{Cl}/X_{OH}) against X_{Mg} plots. The slopes of these linear trends are a function of temperature, but they are independent from pressure and fluid composition, whereas the *y*-intercept value is a function of all these parameters (Zhu and Sverjensky, 1992; Selby and Nesbitt, 2000). The slopes for log (X_F/X_{OH}) against X_{Fe} and log (X_{Cl}/X_{OH}) against X_{Mg} plots were calculated from Equation 23 and 24 of Zhu and Sverjensky (1992). The calculation indicates that the slopes on the log (X_F/X_{OH}) against X_{Fe} diagram change from -2.93 at 100°C to -1.90, -1.25 and -0.858 at 300, 600, and 1000°C, respectively. In comparison, the slopes on the log (X_{Cl}/X_{OH}) against X_{Mg} diagram plots are more gentle and less dependent on the temperature, which change from -1.32 at 100°C to -0.86, -0.56, -0.39 at 300, 600 and 1000°C, respectively (Zhu and Sverjensky, 1992). Using the homogenization temperature (T_h) of 510°C from microthermometric data of fluid inclusions in the early quartz veins/veinlets associated with the early biotite (potassic) alteration zone (Turner, 1995; Garwin, 2000), and temperature stability of mineral assemblages within the transitional chlorite-sericite (intermediate argillic) and proximal actinolite (inner propylitic) alteration zones (475 °C and 290 °C, respectively) (Idrus, 2005), the slopes in this study were determined on the basis of those experimental diagram plots. These calculated slopes pass through the majority of the data points from the central biotite, transitional chlorite-sericite, and proximal actinolite alteration zones (Figure 6).

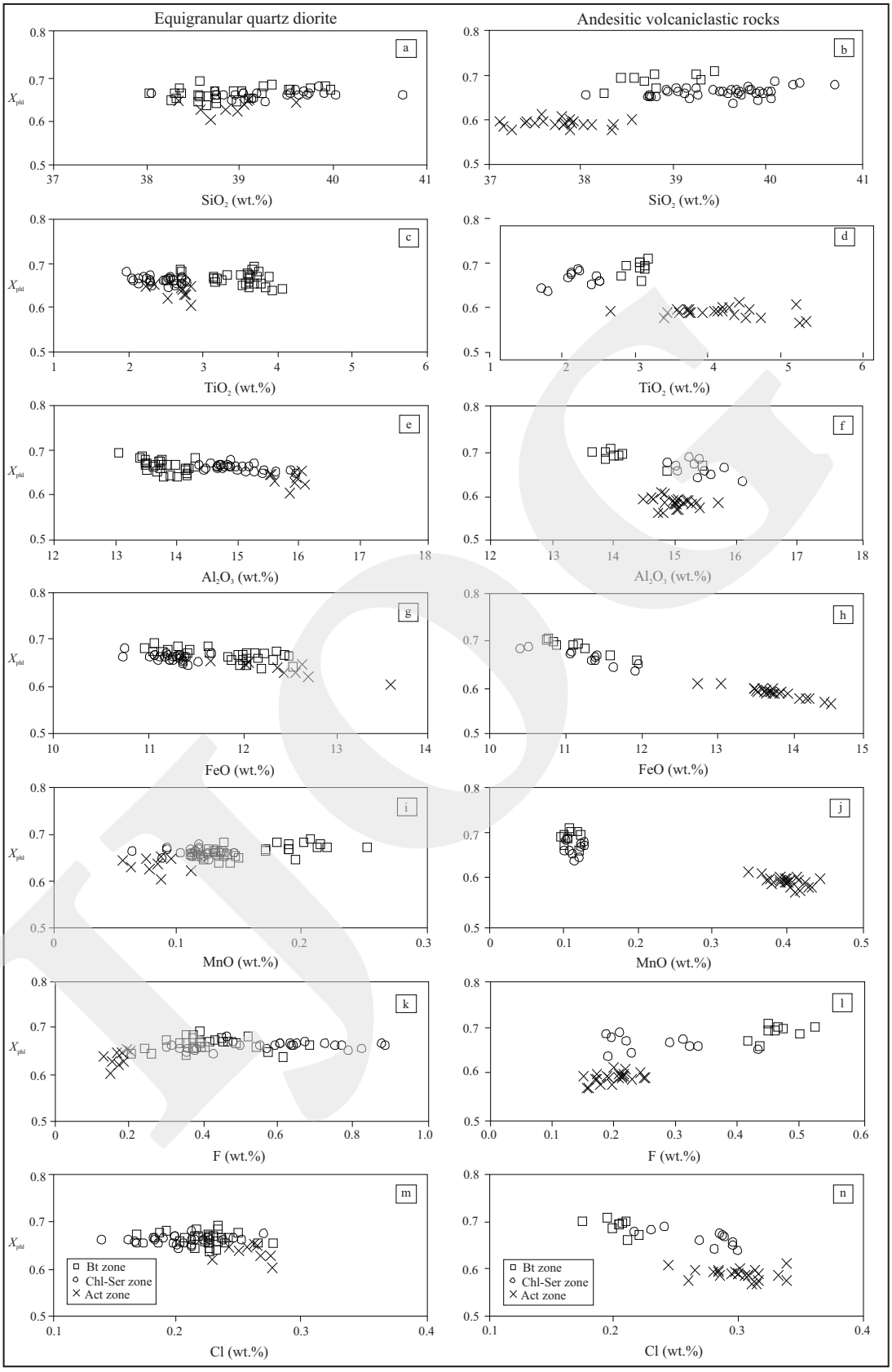

Figure 5. Compositional variations of hydrothermal biotite (N=105) hosted by equigranular quartz diorite (Qde) and andesitic volcaniclastics (Vxl) wall-rocks in three alteration zones comprising central biotite (potassic), transitional chlorite-sericite (intermediate argillic), and proximal actinolite (inner propylitic) zones. N = Number of biotite grains analyzed.

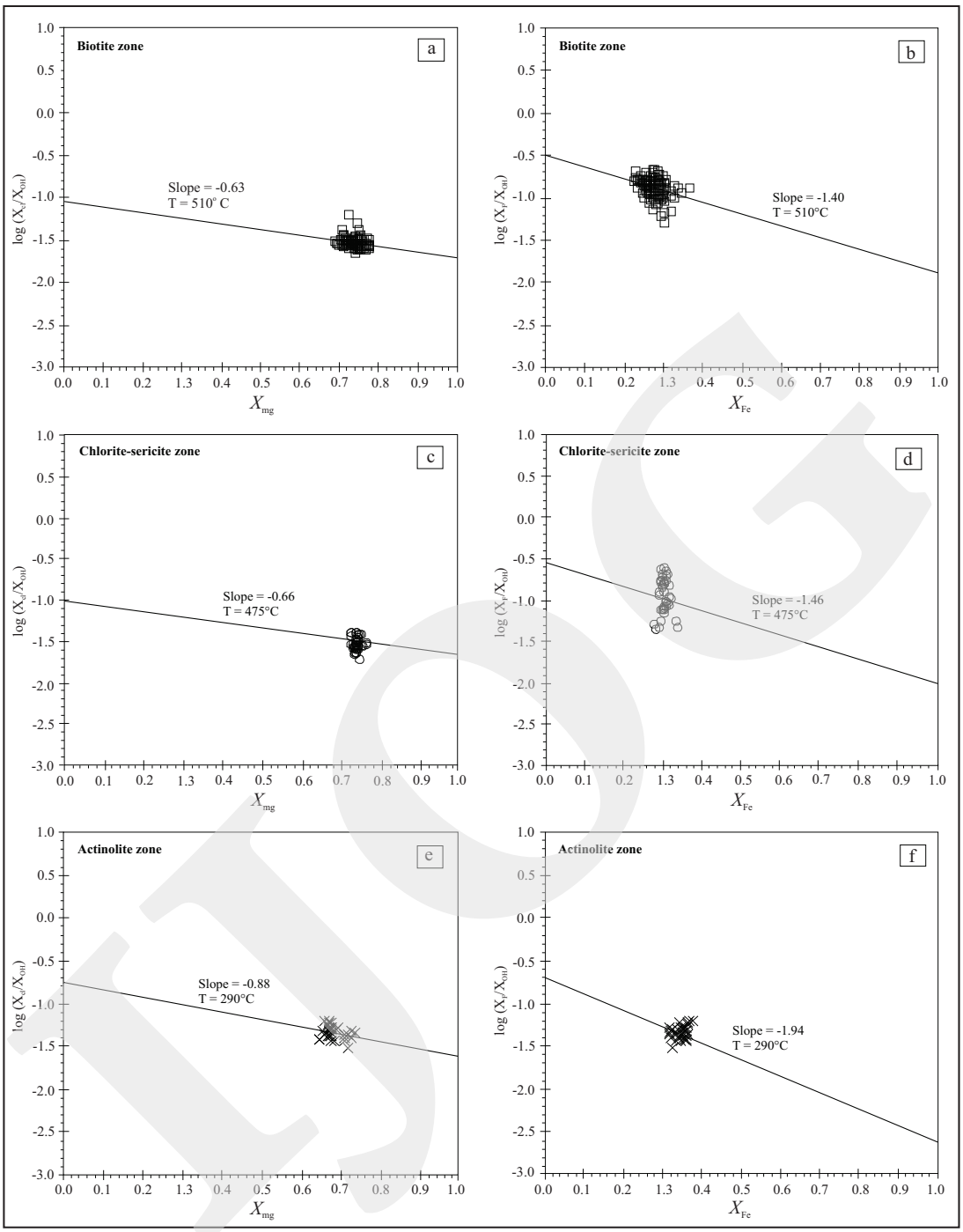

Figure 6. X_{Mg} against log (X_{Cl}/X_{OH}) and X_{Fe} against log (X_F/X_{OH}) plots defining halogen contents of biotite from the three alteration zones: (a) and (b) central biotite (potassic; N = 45), (c) and (d) transitional chlorite-sericite (intermediate argillic; N = 28), and (e) and (f) proximal actinolite (inner propylitic; N=32) alteration zones. Slopes on all plots are derived from the formulations of Zhu and Sverjensky (1991, 1992), and temperatures are from fluid inclusion data and stability of mineral assemblages. Notes: X_F, X_{Cl}, and X_{OH} respectively, represent the mole fractions of F, Cl, and OH in the hydroxyl site, *e.g.* X_F was defined as X_F = F/(F+Cl+OH). N = Number of biotite grains analyzed.

The slopes for the central biotite alteration zone were calculated using maximum Th (510°C) of the fluid inclusions within the early quartz veinlets (Turner, 1995; Garwin, 2000). No microthermometric data are available for the transitional chlorite-sericite and actinolite alteration zones. Therefore, their slopes were defined on the basis of median stability temperatures of those mineral

assemblages. Biotite geothermometry (Beane, 1974) is not applicable, due to the absence of K-feldspar coexisting with biotite within the Batu Hijau deposit. The formation temperatures for the transitional chlorite-sericite and proximal actinolite zones are 475 and 290°C, respectively (Browne, 1978; Clode *et al*., 1999; Garwin, 2002). As a result, the calculated slopes of log (X_{Cl}/X_{OH}) against X_{Mg} and log (X_F/X_{OH}) against X_{Fe} plots for the central biotite alteration zone are -0.63 and -1.40, respectively. The slopes of log (X_{Cl}/X_{OH}) against and X_{Mg} log (X_F/X_{OH}) against X_{Fe} for the transitional chlorite-sericite zone are -0.66 and -1.46 (Figure 6c - d), whereas those for the proximal actinolite zone are -0.88 and -1.94 (Figure 6e - f).

The *y*-intercepts on the log (X_{Cl}/X_{OH}) against X_{Mg} and log (X_F/X_{OH}) against X_{Fe} plots for the central biotite zone are -1.05 and -0.50, respectively (Figure 6a - b). The values are similar to those for the transitional chlorite-sericite zone (-1.00 and -0.55; Figure 6c - d). Some biotite data, particularly log (X_F/X_{OH}) against X_{Fe} for the transitional chlorite-sericite zone (Figure 6d), show a scatter distribution. This may suggest that the biotite compositions were strongly affected by later hydrothermal fluids during alteration. Compared to these alteration zones, the *y*-intercepts on the log (X_{Cl}/X_{OH}) against X_{Mg} and log (X_F/X_{OH}) against X_{Fe} plots for the proximal actinolite zone display different values (-0.75 and -0.70, respectively; Figure 6e - f).

Halogen Fugacity Ratios

The greater exchangeability of elements residing in the hydroxyl site relative to those in the tetrahedral and octahedral sites of biotite opens the possibility that the biotite will undergo F-Cl-OH equilibrium with the hydrothermal fluids that are responsible for the formation of the alteration zones (Selby and Nesbitt, 2000). Mg and Fe contents of the Batu Hijau biotites are directly related to F-Cl-OH exchange between the biotites and hydrothermal fluids, as indicated by a good agreement of their compositions with the "Mg-Cl and F-Fe avoidance rules". The theoretical estimates of F-Cl-OH exchange between biotite and hydrothermal fluids are based on the model equilibrium reaction (Munoz and Ludington, 1974; Gunow *et al*., 1980; Parry *et al*., 1984, and Munoz, 1984):

$$OH_{(biotite)} + HX_{(fluid)} = X_{(biotite)} + H_2O_{(fluid)} \quad \text{.....(1)}$$

where X stands for either F or Cl.

The equilibrium constant is calculated from $\log K = \log (X_X/X_{OH})_{biotite} + \log [(fH_2O)/f(HX)]_{fluid}$. The $\log (X_X/X_{OH})_{biotite}$ portrays the halogen contents of biotite, whereas $\log [(fH_2O)/f(HX)]_{fluid}$ represents the fugacity ratios of the hydrothermal fluids involved. The fugacity ratios consisting of log (fH_2O)/(fHF), log (fH_2O)/(fHCl), and log (fHF)/(fHCl) were further computed using the equations of Munoz (1992), which were based on the revised coefficients for the halogen-hydroxyl exchange (Zhu and Sverjensky, 1991, and 1992). The equations are:

$$\log (fH_2O)/(fHF)_{fluid} = 1000/T[2.37 + 1.1(X_{Mg})_{biotite}] + 0.43 - \log(X_F/X_{OH})_{biotite} \quad \text{.....(2)}$$

$$\log (fH_2O)/(fHCl)_{fluid} = 1000/T[1.15 + 0.55(X_{Mg})_{biotite}] + 0.68 - \log(X_{Cl}/X_{OH})_{biotite} \quad \text{.....(3)}$$

$$\log (fHF)/(fHCl)_{fluid} = -1000/T[1.22 + 1.65(X_{Mg})_{biotite}] + 0.25 + \log(X_F/X_{Cl})_{biotite} \quad \text{.....(4)}$$

Here:

X_F, X_{Cl}, and X_{OH} are mole fractions of F, Cl, and OH in the hydroxyl site of the biotite,

X_{Mg} is the mole fraction of Mg, and

T is the temperature in Kelvin (K) of the halogen-hydroxyl exchange.

The fugacity ratios for hydrothermal fluids associated with the central biotite (potassic), transitional chlorite-sericite (intermediate argillic), and proximal actinolite (inner propylitic) alteration zones were determined at temperatures of 510, 475, and 290°C, respectively (Idrus, 2005). The calculation indicates that the hydrothermal fluids related to the central biotite alteration zone have the average log (fH_2O)/(fHF), log (fH_2O)/(fHCl), and log (fHF)/(fHCl) values of 4.21, 5.39, and

-2.23, respectively. The log (fH_2O)/(fHF) and log (fH_2O)/(fHCl) are slightly lower, and log (fHF)/(fHCl) is relatively similar or slightly higher than those for the fluid related to the transitional chlorite-sericite alteration zone (4.30, 5.64, and -2.43, respectively; Figure 7). The hydrothermal fluids associated with the proximal actinolite alteration zone have the average log (fH_2O)/(fHF), log (fH_2O)/(fHCl), and log (fHF)/(fHCl) values of 4.82, 7.32 and -3.83, respectively. The calculated log (fH_2O)/(fHF) and log (fH_2O)/(fHCl) are considerably higher, and log (fHF)/(fHCl) is typically

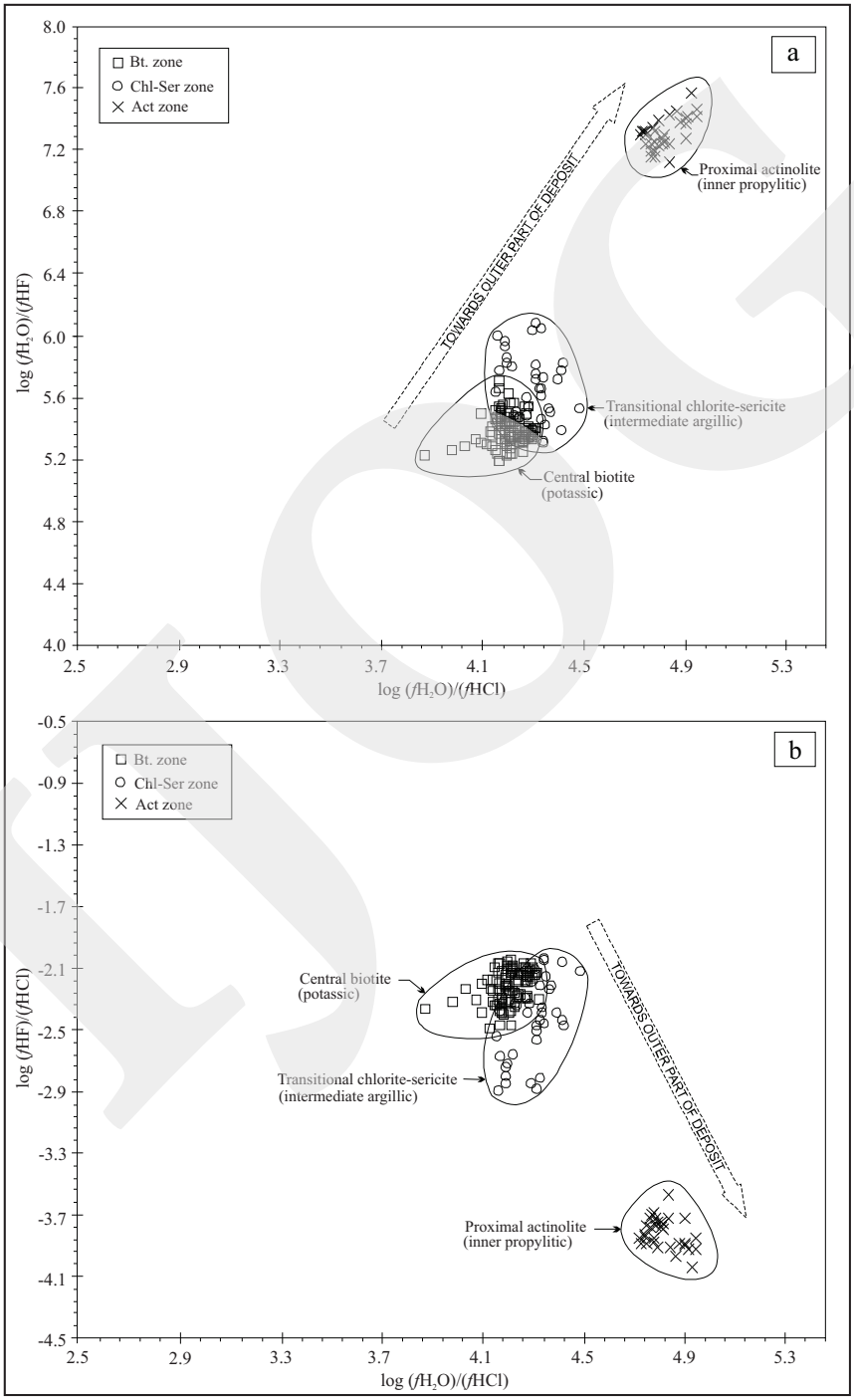

Figure 7. Fugacity ratios of hydrothermal fluids responsible for the formations of central biotite (potassic), transitional chlorite-sericite (intermediate argillic), and proximal actinolite (inner propylitic) alteration zones: (a) log (fH_2O)/(fHCl) against log (fH_2O)/(fHF), and (b) log (fH_2O)/(fHCl) against log (fHF)/(fHCl). Number of hydrothermal biotite grains analyzed (N) = 167.

lower than those related to the central biotite and transitional chlorite-sericite zones (Figure 7). The significant variation in the fugacity ratios for hydrothermal fluids related to the proximal actinolite zone has also been recorded by Selby and Nesbitt (2000) at the Casino porphyry deposit.

Fluid halogen Fugacity: A comparison to other porphyry systems

This section aims to compare the biotite halogen chemistry and halogen fugacity ratios of the hydrothermal fluid responsible for the formation of alteration zones in the Batu Hijau deposit, with those of other major porphyry systems. This allows to better understand the physicochemical conditions of the hydrothermal fluid in the deposit.

The biotite halogen chemistry and halogen fugacity ratios of the hydrothermal fluids related to the central biotite (potassic), transitional chlorite-sericite (intermediate argillic), and proximal actinolite (inner propylitic) alteration zones in the Batu Hijau deposit were compared to those of fluids related to various alteration zones of Bingham (Parry *et al*., 1978; Bowman *et al*., 1987), Santa Rita (Jacobs and Parry, 1979) and Casino (Selby and Nesbitt, 2000) porphyry copper deposits as well as those of fluids associated with the Hanover (Jacobs and Parry, 1976) and Deboullie (Loferski and Ayuso, 1995) porphyry Cu-related plutons (Figure 8). As described in a previous section, the fugacity ratios for hydrothermal fluids associated with the central biotite, transitional chlorite-sericite, and proximal actinolite alteration zones in the Batu Hijau deposit were determined at the temperatures of 510, 475 and 290°C, respectively. The fugacity ratios for other deposits/plutons were recalculated at temperatures established from fluid inclusion or mineral pair geothermometry. The analytical data were taken from related authors above, *e.g.* 350°C for the Santa Rita (potassic alteration), Hanover, and Deboullie as well as 400°C for the Bingham (potassic alteration). The fugacity ratios of the Casino porphyry copper deposit were calculated at temperatures of 420, 390, and 350°C for potassic, phyllic, and propylitic alteration zones (cf. Selby and Nesbitt, 2000).

As outlined before, the hydrothermal fluid related to the central biotite alteration zone in the Batu Hijau deposit have the similar or slightly lower log (fH_2O)/(fHF) and log (fH_2O)/(fHCl) values, and similar or slightly higher log (fHF)/(fHCl) values than those for fluids related to the transitional chlorite-sericite zone. In comparison to other porphyry copper systems, the fluids associated with the central biotite and transitional chlorite-sericite zones possess similar log (fH_2O)/(fHCl) values to those of fluids related to the Santa Rita deposit as well as the Hanover and Deboullie plutons (Figure 8). Log (fH_2O)/(fHCl) values for the central biotite and transitional chlorite-sericite zones of the Batu Hijau are also similar or slightly lower to those of the Bingham deposit. However, the log (fH_2O)/(fHCl) values are slightly higher than those of fluids related to potassic and phyllic alterations in the Casino deposit. Log (fH_2O)/(fHF) values of fluids associated with central biotite and transitional chlorite-sericite zones in the Batu Hijau are similar or slightly lower than those of fluids responsible for the formations of potassic alterations in the Santa Rita and Bingham as well as in phyllic and potassic alterations in the Casino. However, the Batu Hijau log (fH_2O)/(fHF) values are considerably lower than those of fluids related to the Hannover and Deboullie plutons.

In general, the log (fHF)/(fHCl) values of fluids related to all alteration zones in the Batu Hijau are lower compared to those of fluids related to other deposits and plutons, except for Deboullie, which yields relatively similar log (fHF)/(fHCl) values to those of fluid forming the central biotite (potassic) alteration zone in the Batu Hijau deposit. The variability of the fugacity ratios among the porphyry Cu deposits and porphry Cu-related plutons may be directly related to the chemical composition of the exsolved magmatic aqueous fluid. The composition of exsolved magmatic fluids may, in turn, depend on processes, including assimilation and/or fractional crystallisation, which affect the nature of magma(s) on their ascent through the continental crust.

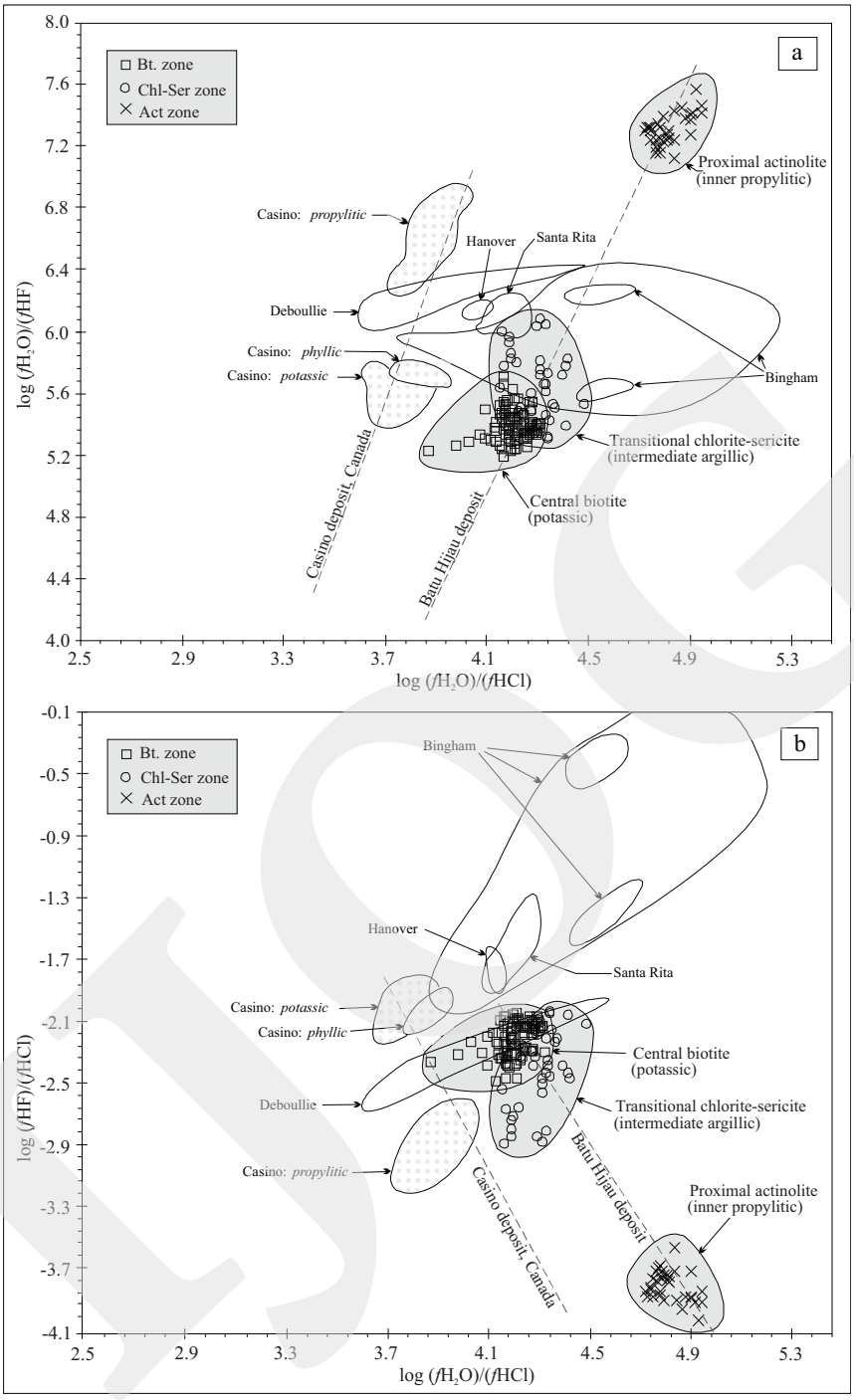

Figure 8. Fugacity ratios of hydrothermal fluids responsible for the formation of the central biotite (potassic), transitional chlorite-sericite (intermediate argillic), and proximal actinolite (inner propylitic) alteration zones within the Batu Hijau deposit and comparison to those of fluids related to alteration zones from the Santa Rita, Bingham, and Casino porphyry Cu deposits as well as from the Hanover and Deboullie porphyry Cu-related plutons: (a) log (fH_2O)/($fHCl$) against log (fH_2O)/(fHF), and (b) log (fH_2O)/($fHCl$) against log (fHF)/($fHCl$). The number of hydrothermal biotite grains analyzed (N) = 167.

In contrast to the hydrothermal fluids related to the central biotite and transitional chlorite-sericite zone, the fluid forming the proximal actinolite (inner propylitic) alteration zone has considerable higher log (fH_2O)/(fHF) and log (fH_2O)/($fHCl$) as well as lower log (fHF)/($fHCl$) values (Figure 8). The similar behaviour is also shown by fluids forming the alteration

zones in the Casino porphyry copper deposit. The fugacity ratios established for potassic and phyllic alteration zones are relatively identical, but the fugacity ratios for propylitic alteration greatly contrast with those for both alteration zones above. Furthermore, log (fH_2O)/(fHF) and log (fH_2O)/(fHCl) values for fluid related to the Casino propylitic zone are typically lower than those for fluid of the Batu Hijau propylitic zone. This suggests that F and Cl contents are higher in the propylitic-related fluid of the Casino than those of Batu Hijau. Interestingly, the trend of the fugacity ratios of fluids related to all alteration zones in both porphyry copper deposits is similar; they increase towards outer parts of the deposits, from central biotite (potassic), transitional chlorite-sericite (intermediate argillic)/phyllic to proximal actinolite (propylitic) alteration zones (Figure 8). This suggests that the halogen contents of hydrothermal fluids in both porphyry copper deposits decrease outward, as a result of a degree increase of mixing between magmatic fluid and meteoric water.

The fugacity ratios determined for potassic alteration at Bingham describe a large range of values (Figure 8a - b). However, the data cluster and with respect to log (fH_2O)/(fHCl) and (fH_2O)/(fHF) define two populations. The large spread in the fugacity ratios at Bingham may suggest that post potassic hydrothermal fluids have modified the biotite halogen chemistry. However, the two populations of the fugacity ratios suggest that two different hydrothermal fluids forming the potassic alteration were present at Bingham. In addition, log (fHF)/(fHCl) values for fluid associated with the potassic alteration zone in the Bingham are significantly higher (-2.0 to -0.1) than those of the fluid determined for the central biotite (potassic) alteration in Batu Hijau (-2.5 to -2.0). This suggets that the magmatic-dominated fluid forming the copper-gold-bearing potassic alteration zone at Bingham has a higher chlorine content than that in fluid related to the central biotite (potassic) alteration zone at the Batu Hijau deposit. The relatively higher chlorine content in the potassic-related fluid at Bingham may reflect a higher activity of chloride complexes in the fluid, in comparison to that at the Batu Hijau deposit.

The chloride complexes have been identified as important components of hydrothermal fluids in transporting copper, gold, and other metals in porphyry deposits (*e.g.* Shinohara, 1994; Gammons and Williams-Jones, 1997). The higher activity of chloride complexes within the potassic-related fluid at Bingham, relative to the Batu Hijau may be expressed by higher average grades of Cu and Au (0.88 % and 0.50 g/t, respectively; Babcock *et al*., 1995 and Keith *et al*., 1997) (Note: the average Cu and Au grades of the Batu Hijau deposit are 0.53 % and 0.40 g/t, respectively; Clode *et al*., 1999).

Conclusions

Biotites in the tonalite porphyries are texturally distinguished into magmatic and hydrothermal types. The magmatic type contains higher TiO_2 and FeO than the hydrothermal type, while F is relatively higher in the hydrothermal biotites. The correlation between X_{Mg} and halogen (F, Cl) contents shows a good agreement with the experimental results of Munoz's (1984). Biotite with high Mg tends to incorporate more F and less Cl compared to biotite with lower Mg; a crystal-chemical effect referred to as "Fe-F and Mg-Cl avoidance rules" (cf. Munoz, 1984; Zhu and Sverjensky, 1991; Munoz, 1992). This suggests that the octahedral Mg and Fe in biotite controls the halogen-hydroxyl exchange of the hydrothermal fluids.

The halogen chemistry of the biotite exhibits a systematic variation through the various alteration zones. The biotite shows a systematic increase in log (X_{Cl}/X_{OH}) values, and a decrease in log (X_F/X_{OH}) and log (X_{Cl}/X_F) values from the early central biotite, transitional chlorite-sericite to the proximal actinolite alteration zones. The y-intercepts on the log (X_{Cl}/X_{OH}) *vs*. X_{Mg} and log (X_F/X_{OH}) *vs*. X_{Fe} plots for biotite from biotite zone (potassic) and chlorite-sericite zone (intermediate argillic) are similar or slightly different. The similarity of

intercepts and the narrow scatter shown in the data for biotite and chlorite-sericite zones imply that the X_F/X_{OH} and X_{Cl}/X_{OH} values of the hydrothermal fluid were fairly constant during the formation of both potassic and intermediate argillic alteration, forming under broadly similar temperature conditions. In contrast, the *y*-intercepts on the log (X_{Cl}/X_{OH}) *vs*. X_{Mg} and log (X_F/X_{OH}) *vs*. X_{Fe} plots for biotite from actinolite zone (inner propylitic) display different values in comparison to both alterations above. The latter suggests that biotite chemistry of the actinolite zone may record the change in fluid composition during the alteration formation. The compositional changes in oxide and halogen chemistry of biotite from the various rocks and alteration types at Batu Hijau deposit conform to those from other porphyry Cu deposits, although absolute concentrations vary considerably among deposits. The narrow variation of the halogen (F, Cl) fugacity ratios in the early central biotite and transitional chlorite-sericite alteration zones may suggest that the hydrothermal fluid composition was fairly constant at a broadly similar temperature. This may also explain the strong overlapping of the early central biotite zone by the transitional chlorite-sericite assemblages. The fugacity ratios increase systematically from the inner, transitional to outer parts of the deposit, corresponding to fluid composition change and relative timing for the subsequent formations of the early, transitional to late alteration zones. High halogen content particularly Cl, contained by hydrothermal biotite may imply that copper and gold in the porphyry deposit were transported in the form of chloride complexes $CuCl_2^-$ and $AuCl_2^-$, respectively.

Acknowledgements

The author is grateful to the Newmont Nusa Tenggara managements for their permission and support during the field works in the Batu Hijau mine. Special thanks are delivered to Steve Garwin, Ph.D. for his enlightenment at the first stage of my study on the Batu Hijau deposit, Adi Maryono and Eddy Priowarsono for his encouragement and fieldwork supervision, respectively. The author is also indebted to DAAD (*Deutscher Akademischer Austauschdienst*) Germany for their financial support for this study. The laboratory work was fully facilitated by RWTH Aachen University, Germany. A sincere gratitude goes to Professor Franz Michael Meyer and Professor Jochen Kolb for their continuous support and collaboration as well as Dr. Annemaria Wiechowski for her precious discussion on biotite chemistry. The author also expresses his thanks to Thomas Derichs and Roman Klinghardt for sample preparation and microprobe analysis assistances, respectively. The latest, but not least, author's appreciation and thanks are expressed to Professor Hiroharu Matsueda and Euis Tintin Yuningsih, Ph.D. for their critical reviews on the manuscript.

References

Afshooni, S.Z., Mirnejad, H., Esmaeily, D., and Asadi Haroni, H., 2013. Mineral chemistry of hydrothermal biotite from the Kahang porphyry copper deposit (NE Isfahan), Central Province of Iran. *Ore Geology Reviews*, 54, p.214-232.

Babcock, R.C., Jr., Ballantyne, G.H., and Phillips, C.H., 1995. Summary of the geology of the Bingham District, Utah. *In*: Pierce, F.W., and Bolm, J.G., (eds), *Porphyry Copper Deposits of the American Cordillera*. Arizona Geological Society Digest, 20, p.316-335.

Bao, B., Webster, J.D., Zhang, D-H., Goldo, B.A., and Zhang, R-Z., 2016. Compositions of biotite, amphibole, apatite and silicate melt inclusions from the Tongchang mine, Dexing porphyry deposit, SE China: Implications for the behavior of halogens in mineralized porphyry systems. *Ore Geology Reviews,* 79, p.443-462.

Beane, R.E., 1974. Biotite stability in the porphyry copper environment. *Economic Geology,* 69, p.241-256.

Bowman, J.R., Parry, W.T., Kropp, W.P., and Kruer, S.A., 1987. Chemical and isotopic evo-

lution of hydrothermal solutions at Bingham, Utah: *Economic Geology*, 82, p.395-428.

Browne, P.R.L., 1978. Hydrothermal alteration in active geothermal fields. *Annual Review of Earth and Planetary Sciences,* 6, p.229-250.

Clode, C., Proffett, J., Mitchell, P., and Munajat, I., 1999. Relationships of Intrusion, Wall-Rock Alteration and Mineralisation in the Batu Hijau Copper-Gold Porphyry Deposit. *Proceedings, Pacrim Congress, Bali-Indonesia*, p.485-498.

Gammons, C.H. and Williams-Jones, A.E., 1997. Chemical mobility of gold in the porphyry-epithermal environment. *Economic Geology,* 92, p.45-59.

Garwin, S.L., 2000. *The setting, geometry and timing of intrusion-related hydrothermal systems in the vicinity of the Batu Hijau porphyry copper-gold deposit, Sumbawa, Indonesia*. Unpublished *Ph.D Thesis*, University of Western Australia, Perth, 320pp.

Garwin, S.L., 2002. The Geologic Setting of Intrusion-Related Hydrothermal Systems near the Batu Hijau Porphyry Copper-Gold Deposit, Sumbawa, Indonesia. *Global Exploration Integrated Methods for Discovery*, Colorado, USA. *Society of Economic Geologists Special Publication,* 9, p.333-366.

Gunow, A.J., Ludington, S., and Munoz, J.L., 1980. Flourine in micas from the Henderson molybdenite deposit, Colorado. *Economic Geology,* 75, p.1127-1137.

Idrus, A., 2005. *Petrology, Geochemistry and Composional Changes of Diagnostic Hydrothermal Mineral Within the Batu Hijau Porphyry Copper-Gold Deposit, Sumbawa Island, Indonesia*. Unpublished *Doctor Dissertation*, RWTH Aachen University, Germany, 352 pp.

Idrus, A., Kolb, J., and Meyer, F.M., 2007. Chemical composition of rock-forming minerals in copper-gold-bearing tonalite porphyry intrusions at the Batu Hijau deposit, Sumbawa Island, Indonesia: Implications for crystallisation conditions and fluorine-chlorine fugacity. *Resource Geology,* 57, p.102-113.

Jacobs, D.C. and Parry, W.T., 1976. A comparison of the geochemistry of biotite from some basin and range stocks. *Economic Geology,* 71, p.1029-1035.

Jacobs, D.C. and Parry, W.T, 1979. Geochemistry of biotite in the Santa Rita porphyry copper deposit, New Mexico. *Economic Geolology,* 74, p.860-887.

Keith, J.D., Whitney, J.A., Hattori, K., Ballantyne, G.H., Christiansen, E.H., Barr, D.L., Cannan, T.M., and Hook, C.J., 1997. The role of magmatic sulphides and mafic alkalinemagmas in the Bingham and Tintic mining districts, Utah. *Journal of Petrology,* 38, p.1679-1690.

Loferski, P.J. and Ayuso, R.A., 1995. Petrology and mineral chemistry of the composite Deboullie pluton, northern Maine, USA: Implication for the genesis of Cu-Mo mineralisation. *Chemical Geology,* 123, p.89-105.

Moradi, R., Boomeri, M., Bagheri, S., and Nakashima, K., 2016. Mineral chemistry of igneous rocks in the Lar Cu-Mo prospect, southeastern part of Iran: implications for P, T, and $fO2$. *Turkish Journal of Earth Sciences,* 25, p.418-433.

Munoz, J.L., 1984. F-OH and Cl-OH exchange in micas with applications to hydrothermal ore deposits. *Reviews in Mineralogy,* Bailey, S.W., eds., 13, p.469-494.

Munoz, J.L., 1992. Calculation of HF and HCl fugacities from biotite compositions: revised equations. *Geological Society of America, Abstract Programs,* 24, A221.

Munoz, J.L. and Ludington, S.D., 1974. Fluoride-hydroxil exchange in biotite. *American Journal of Science,* 274, p.396-413.

Munoz, J.L. and Swenson, A., 1981. Chloride-hydroxyl exchange in biotite and estimation of relation HCl/HF activities in hydrothermal fluids. *Economic Geology,* 76, p.2212-2221.

Parry, W.T., Ballantyne, J.M., and Jacobs, D.C., 1984. Geochemistry of hydrothermal sericite from Roosevelt Hot Springs and the Tictic and Santa Rita porphyry copper systems. *Economic Geology,* 79, p.72-86.

Parry, W.T., Ballantyne, G.H., and Wilson, J.C., 1978. Chemistry of biotite and apatite from

a vesicular quartz latice porphyry plug at Bingham, Utah. *Economic Geology,* 73, p.1308-1314.

Parry, W.T. and Jacobs, D.C., 1975. Flourine and chlorine in biotite from Basin and Range plutons. *Economic Geology,* 70, p.554-558.

Rieder, M., Cavazzini, G., D`Yakonov, Y.S., Frank-Kamentskii, V.A., Gottardi, G., Guggenheim, S., Koval, P.V., Müller, G., Neiva, A.M.R., Radoslovich, E.W., Robert, J-L., Sassi, F.P., Takeda, H., Weiss, Z., and Wones, D.R., 1998. Nomenclature of the micas. *The Canadian Mineralogist,* 36, p.41-48.

Selby, D. and Nesbitt, B.E., 2000. Chemical composition of biotite from the Casino porphyry Cu-Au-Mo mineralisation, Yukon, Canada: evaluation of magmatic and hydrothermal fluid chemistry. *Chemical Geology,* 171, p.77-93.

Shinohara, H., 1994. Exsolution of immiscible vaper and liquid phases from a crystallizing silicate melt: Implications for chlorine and metal transport. *Geochimica et Cosm chimica Acta,* 58, p.5215-5221.

Turner, S.J., 1995. Fluid inclusion study of Batu Hijau porphyry Cu-Au deposit, Southwest Sumbawa, Indonesia: implications for mineralisation and metal patterns around a major porphyry stock. Unpublished Newmont Nusa Tenggara company report, 49pp.

Zhang, W., Lentz, D.R., Thorne, K.G., and McFarlane, C., 2016. Geochemical characteristics of biotite from felsic intrusive rocks around the Sisson Brook W-Mo-Cu deposit, west-central New Brunswick: An indicator of halogen and oxygen fugacity of magmatic systems. *Ore Geology Reviews,* 77, p.82-96.

Zhu, C. and Sverjersky, D.A., 1991. Partitioning of F-Cl-OH between minerals and hydrothermal fluids. *Geochimica et Cosmochimica Acta,* 55, p.1837-1858.

Zhu, C. and Sverjersky, D.A., 1992. Partitioning of F-Cl-OH between biotite and apatite. *Geochimica et Cosmochimica Acta,* 56, p.3435-3467.